Changes in structure and properties due to mechanical fatigue for polyurethanes containing poly(dimethyl siloxane)

Shinichi Sakurai*, Satoshi Nokuwa, Masato Morimoto, Mitsuhiro Shibayama and Shunji Nomura

Department of Polymer Science and Engineering, Kyoto Institute of Technology, Matsugasaki, Sakyo-ku, Kyoto 606, Japan

(Received 3 March 1993; revised 17 May 1993)

Changes in structure and properties due to mechanical fatigue for segmented polyurethanes containing a block segment of poly(ethylene oxide)-*block*-poly(dimethyl siloxane)-*block*-poly(ethylene oxide) (PES) were investigated by mechanical and thermal analyses and a small-angle X-ray scattering (SAXS) technique. Six types of specimens designated KP-*x*-*y* were studied, where *x* and *y* denote, respectively, the fraction of PES component ($x=0$ or 13 wt%) and the molecular weight of the soft-segment block, poly(tetramethylene glycol) (PTMG) ($y=1000$, 2000 or 3000). The SAXS experiments revealed that dissociation of the hard-segment microdomains was induced by mechanical fatigue. The changes in the mechanical properties due to fatigue were discussed in relation to the PTMG soft-segment crystallization which can be triggered by the dissociation of the hard-segment microdomains. As already reported, KP-13-2000 has better antithrombogenicity and more suitable viscoelastic properties for use as a biomedical material than any of the others. It was found in this study that KP-13-2000 has strong resistance against mechanical fatigue as well, which is one of the most important characteristics required for biomedical materials. Although the microdomain structure was fractured by fatigue, the mechanical property of KP-13-2000 was not changed because the PES component prevents the PTMG soft segments from crystallizing.

(Keywords: polyurethanes; mechanical fatigue; microdomains)

INTRODUCTION

Segmented polyurethane (SPU) and segmented poly(urethane urea) (SPUU) are widely used as biomedical materials, particularly for artificial hearts and blood vessels, since they have antithrombogenicity and suitable mechanical properties for these purposes[1,2]. The structures, mechanical and thermal properties, surface characterization and blood compatibility of SPU and SPUU have been studied in order to improve properties for biomedical use, by means of a variety of techniques, such as dynamic viscoelastic measurement, differential scanning calorimetry, scanning electron microscopy, transmission electron microscopy, X-ray photoelectron spectroscopy, small-angle X-ray scattering (SAXS), wide-angle X-ray diffraction, and infra-red spectroscopy[3–20].

The characteristic properties such as antithrombogenicity and the elastomeric nature of SPU and SPUU can result from microphase separation between the different types of components in a block copolymer chain. For example, an SPU comprising 1,4-diphenylmethane diisocyanate (MDI) as a hard segment and poly(tetramethylene glycol) (PTMG) as a soft segment is a multiblock copolymer and therefore forms microphase-separated structures due to the strong segregation between soft and hard segments. Since the hard-segment microdomains act as crosslinks for flexible PTMG chains, the SPU exhibits elastomeric properties. It has been reported by Kira *et al.*[21] that better antithrombogenicity is attained when the soft segment contains poly(dimethyl siloxane) (PDMS) which unfavourably degrades mechanical properties due to microphase mixing. Since long-term stability *in vivo* is also required for biomedical use, changes in properties due to fatigue behaviour should be elucidated for SPU and SPUU. Takahara *et al.*[6] have reported partial microphase mixing and orientation of hard and soft segments for fatigued SPU. They also reported changes in structure and properties for SPUU caused by fatigue after lipid sorption in order to examine the effect of fatigue in a biological environment[13] and stated that the effect of fatigue was more pronounced in the case of the weaker cohesive force between the hard segments. Shibayama *et al.*[14–17] studied the morphological and orientational changes due to mechanical fatigue in air and in an aqueous environment in order to elucidate the fatigue mechanism in SPUU. They also reported the progress of microphase mixing and reduction of cohesive force between the hard segments due to fatigue by evaluating a degree of hydrogen bonding using Fourier transform infra-red spectroscopy.

In a previous paper[20] we examined the mechanical and thermal properties and some aspects of the structure of the SPU specimen containing a block segment of poly(ethylene oxide)-*block*-poly(dimethyl siloxane)-*block*-poly(ethylene oxide) (PES), coded as KP-*x*-*y*, by focusing on the degree of completion of microphase

*To whom correspondence should be addressed

0032-3861/94/030532–08

separation and the capability of crystallization of PTMG soft segments. The specimens KP-*x*-*y*, where *x* and *y* denote the fraction of the PES component ($x=0$ or 13 wt%) and the molecular weight of the PTMG soft segments ($y=1000$, 2000 or 3000), respectively, were synthesized by Kanegafuchi Co. Ltd. The SAXS analyses indicated that the size of the soft segment matrix obeys the 2/3-power rule for the molecular weight and that the hard-segment domain size is ~70 Å irrespective of M_{PTMG}, where M_{PTMG} stands for the average molecular weight of a PTMG block chain. Surface enrichment of KP-13-2000 was also detected in the blends of KP-13-2000 and KP-0-2000, which might be applied to surface property modification of a polymer film by blending.

In this study, changes in structure and mechanical properties due to mechanical fatigue for these specimens, KP-*x*-*y*, were investigated by mechanical and thermal analyses and a SAXS technique. The SAXS experiments were conducted to detect the dissociation of the hard-segment microdomains induced by mechanical fatigue. Changes in the mechanical properties due to fatigue were then discussed in relation to the crystallization of the PTMG soft segments which may be triggered by dissociation of the hard-segment microdomains. We have already reported in a previous paper[19] that an introduction of 13 wt% PES component to the soft segment in order to improve antithrombogenicity does not significantly affect the mechanical and thermal properties. Thus, KP-13-2000 turned out to have both antithrombogenicity and suitable viscoelastic properties for biomedical materials. In this paper, special attention is paid to the resistance against mechanical fatigue for this KP-13-2000 to examine long-term stability *in vivo*, which is one of the most important characteristics required for biomedical materials.

EXPERIMENTAL

Chemical structures of the KP-0 and KP-13 series are shown in *Figure 1*. These specimens were supplied by Kanegafuchi Chemical Industry Co. Ltd. The KP-13 series contain 13 wt% of the PES component. The average degrees of polymerization of poly(ethylene oxide) (PEO) and PDMS blocks in PES are 15 and 14, respectively, which give the number-average molecular weight of 2400 for PES. The hard (MDI-EG) where EG denotes ethylene glycol, to soft (PTMG) segment ratio was kept constant for all specimens. The fraction of MDI+EG was kept at 32 wt%. The number-average molecular weights of PTMG, M_{PTMG}, were 1025, 2000 and 2950 for KP-*x*-*y* specimens having $y=1000$, 2000 and 3000, respectively. The heterogeneity indices for the PTMG molecular weight (M_w/M_n, where M_n and M_w are number- and weight-average molecular weights, respectively) were measured by gel-permeation chromatography (g.p.c.) and were 1.89, 2.00 and 2.13 for the KP-*x*-*y* specimens having $y=1000$, 2000 and 3000, respectively. More details of the sample preparation are given elsewhere[21]. Film specimens were obtained by casting from solvent using a mixture of *N*,*N*′-dimethyl acetamide/1,4-dioxane (30/70 by volume). The as-cast films were then dried in a vacuum oven kept at 60°C for three days. The thickness of the as-cast film was approximately 70 μm.

The as-cast specimens, 50 mm long and 10 mm wide, were subjected to mechanical fatigue carried out by

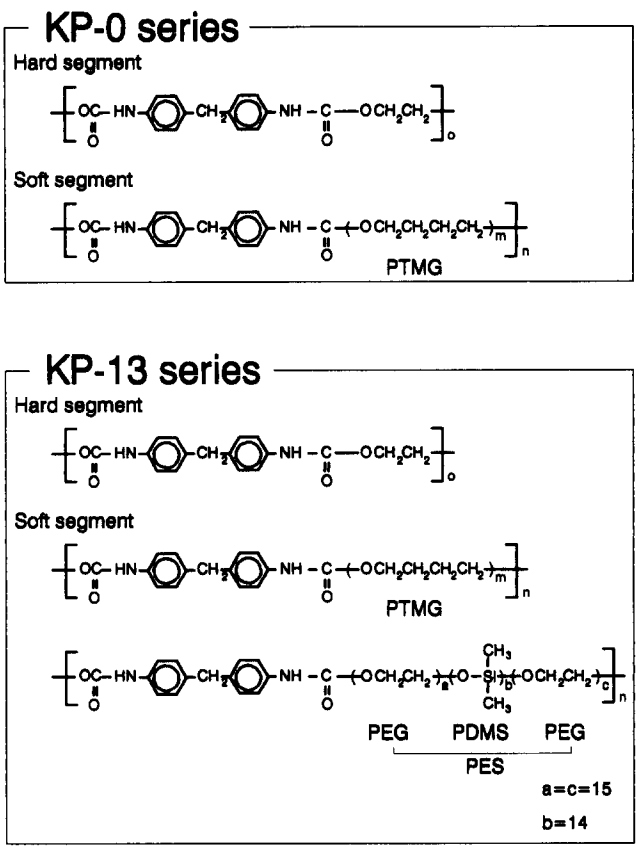

Figure 1 Chemical structure of KP-0 and KP-13 series

applying a 20% dynamic sinusoidal strain in addition to a 100% static strain at a rate of 10 Hz for 10^5 s at 20°C and 40% relative humidity. The details of the fatigue-testing apparatus are given elsewhere[14]. The fatigued film specimens were then stored in a desiccator until used.

Dynamic viscoelastic (DVE) behaviours were examined on film specimens 5 mm wide and 20 mm long with a Rheospectoler DVE-V4 (Rheology Co. Ltd). A synthesized wave comprising eight strain frequencies of 2^n Hz, where *n* is an integer ($n=0$–7), was used for the measurement under a constant temperature scan with the heating rate of 3°C min^{-1}. In this paper, only temperature dispersion at 128 Hz is presented. The temperature range was −150 to 150°C.

Differential scanning calorimetry (d.s.c.) was conducted using a DSC 3100, (MAC Science Co. Ltd). The temperature range was −150 to 150°C. The heating rate was 5°C min^{-1}. During the experiment, the sample was purged by nitrogen gas.

In order to characterize the microdomain structures in very thin fatigued films, an X-ray source with super high intensities was required. Hence, SAXS measurements were performed using synchrotron radiation as an X-ray source at the BL-10C beam line in the Photon Factory of the National Laboratory for High Energy Physics, Japan. The incident beam was focused with a bent cylindrical mirror and monochromatized with a pair of Si(1 1 1) crystals. The wavelength λ of the incident beam was 1.488 Å. The film specimens were exposed to the X-ray beam for about 300 s in such a way that the film normal was parallel to the propagation direction of the incident beam (through view). The scattered intensity was collected at room temperature with a one-dimensional

position-sensitive proportional counter. The sample-to-detector distance was 1.9 m. The details of the apparatus are given elsewhere[22,23]. The measured scattered intensity was further corrected for air-scattering, for absorption due to the specimen, and for thickness of the specimens.

RESULTS AND DISCUSSION

Changes in properties with time after cessation of fatigue

In *Figure 2*, the temperature dependence of storage modulus, E', and loss tangent, $\tan\delta$, were presented for KP-0-2000 as a function of time after cessation of the mechanical fatigue. First of all, let us divide the temperature dependence of the as-cast film into three regions in accordance with the previous work[20]. The E' value decreases gradually with temperature from 6×10^3 to 2×10^3 MPa in the temperature range from -150 to -75°C (region I). In this region, there is an obvious peak at -130°C in $\tan\delta$, corresponding to the amorphous relaxation due to the local motions of methylene groups of the main chain[24,25]. In the following region II from -75 to 20°C, the value of E' falls to 20 MPa at around 20°C. There was a peak in $\tan\delta$ at $-40\sim-35$°C which can be taken as the glass transition temperature, T_g, of the PTMG soft segment. The values of E' and $\tan\delta$ showed no pronounced change with temperature in region III from 20 to 150°C. It is worth pointing out that KP-0-2000 exhibited a rubbery plateau up to 150°C with plateau modulus E' of approximately 15 MPa in region III.

Now let us discuss the time dependence of the dynamic mechanical properties. There are obvious changes only in region II, which seem to achieve a steady state within 72 hours after cessation of mechanical fatigue. As the time increased, the storage modulus E' in the region from -50 to 5°C increased, the peak height of $\tan\delta$ at $-40\sim-35$°C decreased and a distinct shoulder appeared at around -8°C. The lowering of the $\tan\delta$ peak at $-40\sim-35$°C indicates a decrease in the quantity of the amorphous PTMG chains. The appearance of the $\tan\delta$ shoulder at around -8°C can be attributed to the melting of PTMG crystallites. These phenomena strongly suggest an increase of the PTMG crystallites which were formed during the cooling process for the DVE measurements. In consequence, the value of the storage modulus was increased in the range from -50 to 5°C by mechanical fatigue. Based on these results, it is considered that the PTMG chains which were restrained from crystallizing by the hard-segment microdomains in the as-cast film became mobile enough to crystallize due to dissociation of the hard-segment microdomains by the mechanical fatigue. Moreover, it is suggested by the results shown in *Figure 2* that the crystallizability of the PTMG chains within the cooling process increased with time after the cessation of the mechanical fatigue. In the fatigued specimen, small PTMG crystallites may be formed at room temperature and the number of the crystallites may gradually increase with time. Since the small crystallites in turn behave as nuclei for the crystal growth in the cooling process prior to the successive DVE measurements, the crystallizability of the PTMG chains in the region II may increase with time. As a matter of fact, similar behaviour of E' and $\tan\delta$ in region II has been observed with increasing the crystallizability of the PTMG chains through decreasing the cooling rate for the DVE measurement of the non-fatigued KP-0-3000 in a previous work (see Figure 5 in ref. 20).

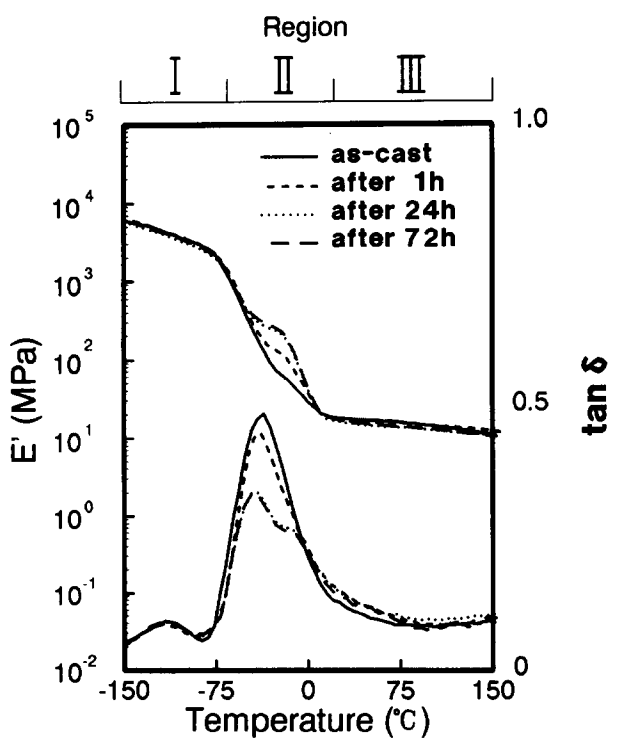

Figure 2 Temperature dependence of storage modulus, E', and loss tangent, $\tan\delta$ of KP-0-2000 as a function of time after cessation of the mechanical fatigue

Changes in properties due to fatigue

We are now in a position to elucidate changes in mechanical and thermal properties due to mechanical fatigue. Based on the results discussed in the previous section, the fatigued film achieved a steady state within 72 hours of cessation of the fatigue. Therefore, results of the fatigued films at 72 hours after the fatigue are used in the following discussion. *Figures 3–5* show the temperature dependences of the storage moduli E' and $\tan\delta$ of the as-cast and fatigued films for the KP-0 and KP-13 series. No obvious difference between the as-cast and fatigued films can be detected for KP-0-1000, KP-13-1000 and KP-13-2000. On the other hand, as discussed above for KP-0-2000, the storage modulus in the region of -50 to 5°C increased, the peak height of $\tan\delta$ at $-40\sim-35$°C decreased and a distinct shoulder appeared at around -8°C.

For KP-0-3000 and KP-13-3000, the change due to fatigue is striking. The storage modulus E' increased in the temperature range from -75°C to 30°C, and the peak in $\tan\delta$ at around -30°C disappeared and the value of $\tan\delta$ increased in the range from 0 to 30°C for the fatigued KP-0-3000 and KP-13-3000 films as compared with the corresponding as-cast films. The disappearance of the $\tan\delta$ peak indicates a drastic decrease in the quantity of the amorphous PTMG chains. The increase of $\tan\delta$ value in the range from 0 to 30°C can be attributed to the melting of PTMG crystallites. These phenomena strongly suggest the existence of crystallites of PTMG in the fatigued specimens even at room temperature, which is discussed later in *Figure 6*. In consequence, the value of the storage modulus was increased by a factor of 3–4 at around 30°C by mechanical fatigue.

Finally, it should be pointed out that the E' values in

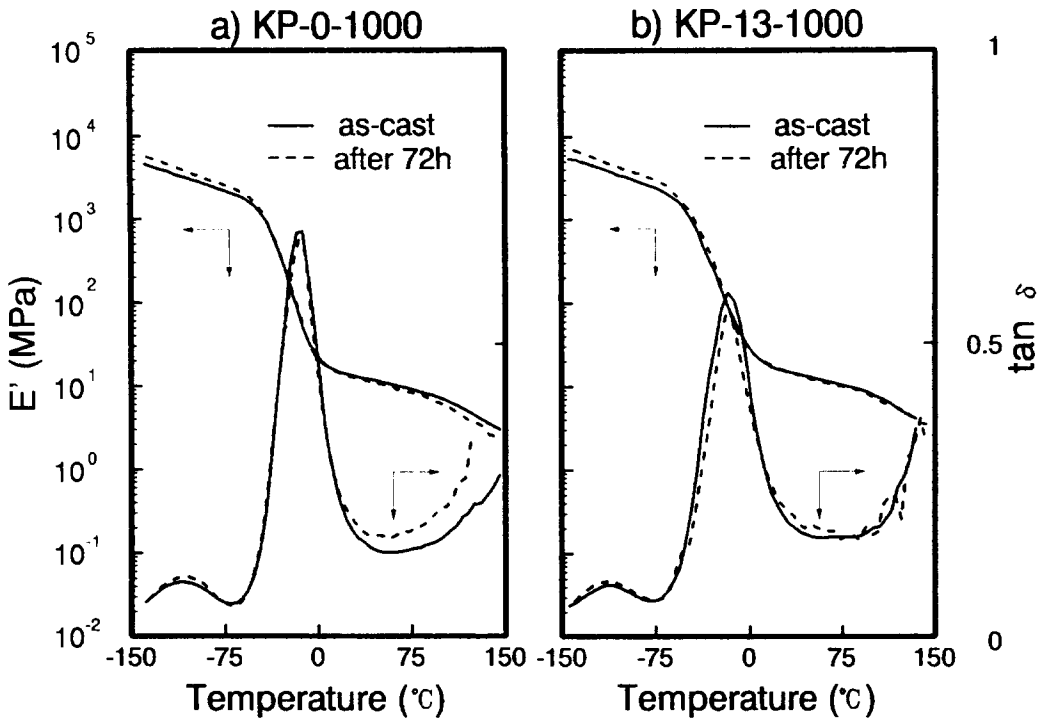

Figure 3 Temperature dependence of the storage modulus E' and tan δ of the as-cast and fatigued films for (a) KP-0-1000 and (b) KP-13-1000

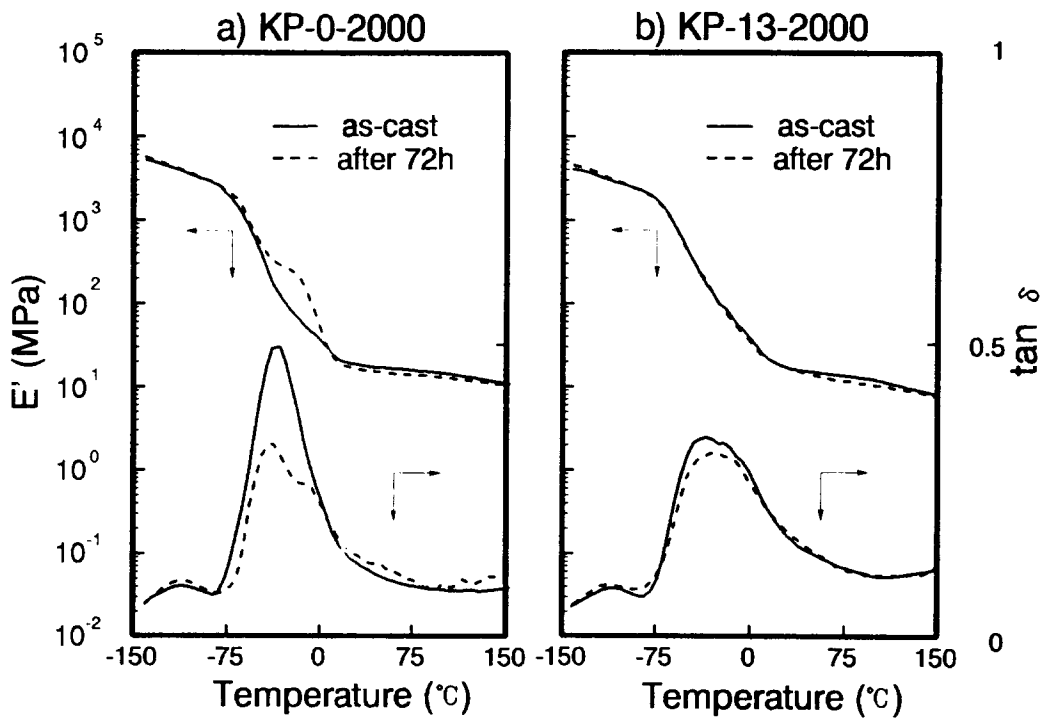

Figure 4 Temperature dependence of the storage modulus E' and tan δ of the as-cast and fatigued films for (a) KP-0-2000 and (b) KP-13-2000

the region from 30 to 150°C do not markedly change due to fatigue for all specimens. Takahara *et al.*[6] reported that the E' values in this temperature range were lowered by a factor of one-tenth by mechanical fatigue for their SPUU which had a comparatively weak cohesive force between the hard segments. They also reported that the E' values did not change very much in the case of SPUU having a comparatively strong cohesive force between the hard segments. Therefore, the cohesive force between the hard segments in our specimens can be stated to be comparatively strong.

Figure 6 shows the d.s.c. thermograms of the as-cast (solid curve) and fatigued (broken curve) films for KP-0-3000 and KP-13-3000, where $T_{g,s}$ stands for the glass transition temperature for the PTMG soft segment. For the as-cast film, crystallization of the soft segments,

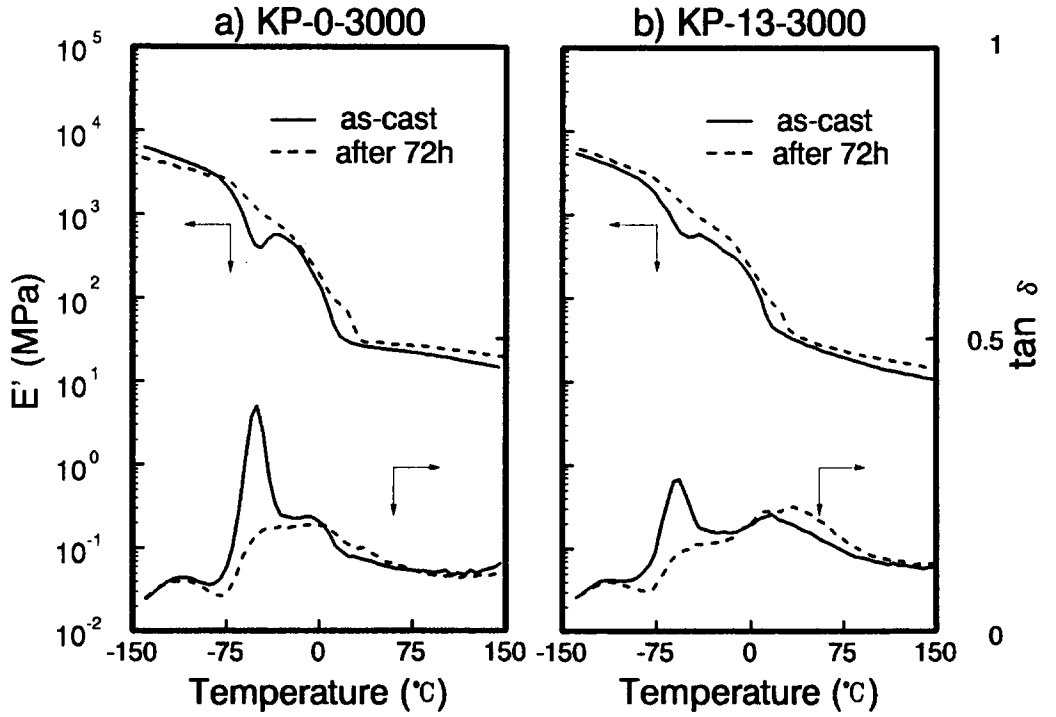

Figure 5 Temperature dependence of the storage modulus E' and tan δ of the as-cast and fatigued films for (a) KP-0-3000 and (b) KP-13-3000

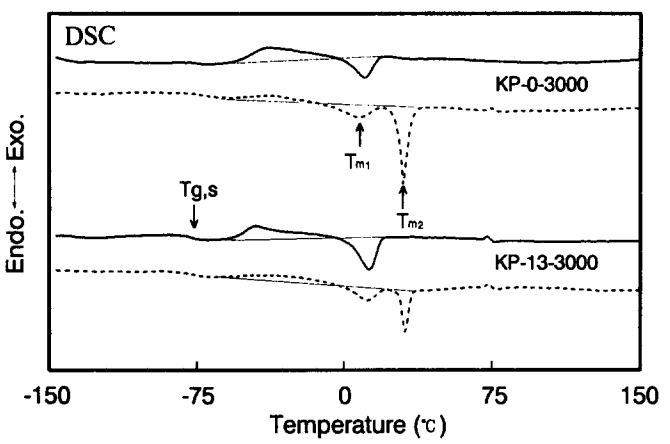

Figure 6 D.s.c. thermograms of the as-cast (——) and fatigued (– – –) films for KP-0-3000 and 13-3000, where $T_{g,s}$ stands for the glass transition temperature for the soft segment and T_{m1} and T_{m2} are the melting temperatures of PTMG crystallites

quenched without crystallizing in the rapid cooling process for the successive d.s.c. experiment, occurred at around $-60 \sim -5$°C and was followed by melting at T_{m1} at around 0–20°C. For the fatigued specimens, additional significant endothermic peaks were detected at T_{m2} at around 30°C for both KP-0-3000 and KP-13-3000, indicating the existence of PTMG crystallites at T_{m2}. It can be considered that the PTMG chains which were restrained from crystallizing by the hard-segment microdomains in the as-cast film became mobile enough to crystallize due to the dissociation of the hard-segment microdomains by the fatigue.

Changes in microdomain structures due to fatigue

The SAXS profiles (the measured scattered intensity as a function of the magnitude of scattering vector, $q \equiv |\mathbf{q}|$, defined by equation (1)) are shown in *Figures 7–10* in semilogarithmic plots of the scattered intensity, $I(q)$, vs. q which is given by:

$$q = (4\pi/\lambda)\sin(\theta/2) \quad (1)$$

with θ and λ being the scattering angle and the wavelength of X-rays ($\lambda = 1.488$ Å), respectively. These profiles were all obtained at ~ 35°C. It should be mentioned that there is no crystalline region at this measuring temperature, which is obvious from the d.s.c. results shown in *Figure 6*, so that the scattering can be attributed to the microphase-separated structures. Before discussing the change due to fatigue, let us briefly summarize the change in microdomain structure with the molecular weight of the soft segment for the as-cast films of the KP-0 and KP-13 series, which have already been reported[20]. The SAXS profiles for the as-cast films are presented in *Figure 7*. It was found that the scattering maximum exhibits a systematic change with M_{PTMG}. The scattering maximum shifts towards the smaller angle region with an increase of M_{PTMG}, indicating that the average of the interdomain distance increases with increasing M_{PTMG}. Moreover, the peak height increases with the increase of M_{PTMG}, suggesting that the degree of completion in the microphase separation is better for the larger M_{PTMG}.

Figures 8 and *9* show the SAXS profiles for the as-cast and fatigued films for KP-0-1000, KP-13-1000, KP-0-3000 and KP-13-3000. For the fatigued films, the profiles taken in the directions parallel and perpendicular to the mechanical fatigue are presented. Hereafter the former is referred to as fatigue-$\parallel$ and the latter as fatigue-$\perp$. The peak intensity decreased due to the mechanical fatigue and peak shifts can be seen towards the smaller and larger angle regions for fatigue-$\parallel$ and fatigue-$\perp$, respectively. These results indicate that the dissociation of the hard-segment microdomains and microphase mixing were induced by the mechanical fatigue and that the resulting structure was anisotropic, that is, compared with

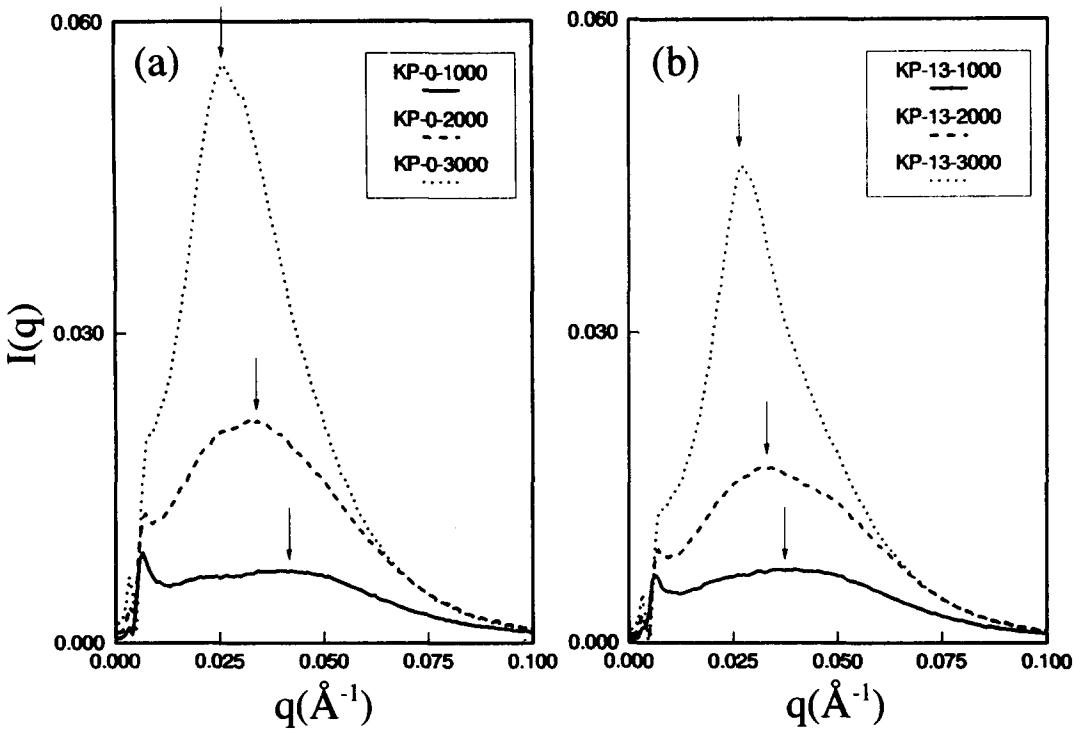

Figure 7 SAXS profiles for the as-cast films for (a) KP-0 series and (b) KP-13 series

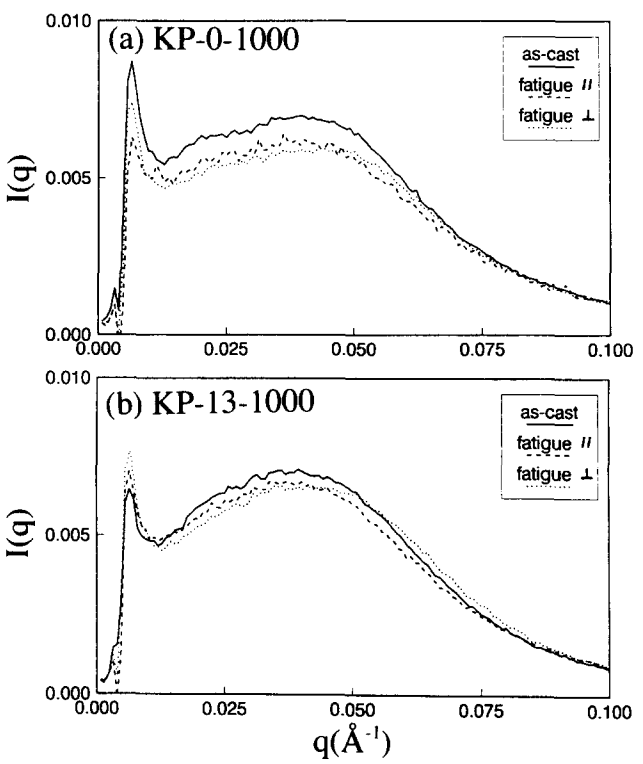

Figure 8 SAXS profiles for the as-cast and fatigued films for (a) KP-0-1000 and (b) KP-13-1000. Fatigue-|| and fatigue-⊥ for the fatigued films denote the profiles taken in the directions parallel and perpendicular to the mechanical fatigue, respectively

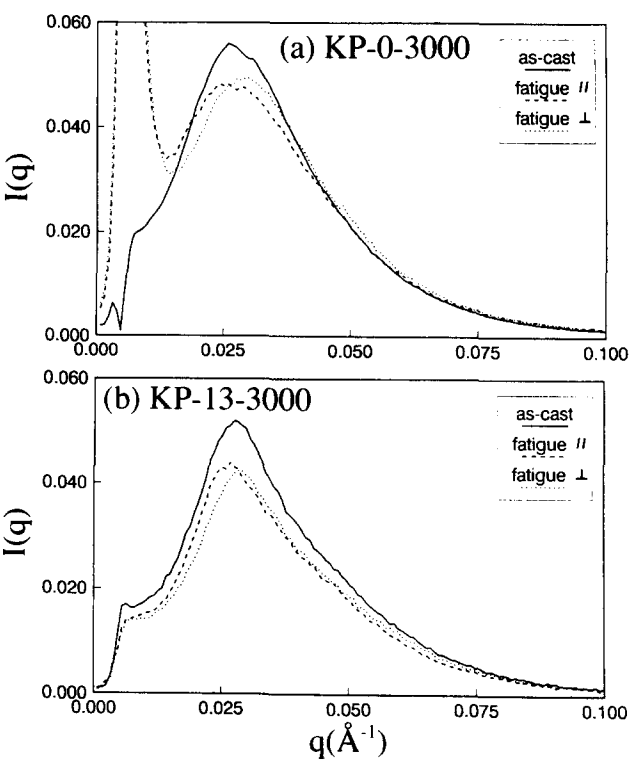

Figure 9 SAXS profiles of the as-cast and fatigued films for (a) KP-0-3000 and (b) KP-13-3000. See the notation for fatigue-|| and fatigue-⊥ in *Figure 8*

the structure of the as-cast film, the average interdomain distances for the fatigued specimen are longer and shorter, respectively, in the directions parallel and perpendicular to the applied fatigue. Since dissociation of the hard-segment microdomains was observed for the specimens having $M_{PTMG} = 1000$ and 3000, such dissociation by mechanical fatigue may be considered for the specimens having $M_{PTMG} = 2000$ as well.

Here, it is useful to elucidate changes in the microdomain structure with uniaxial strain. The change is shown in *Figure 10a* for the case where the scattering vector **q** is parallel to the uniaxial strain (**q**|| strain) for KP-13-3000.

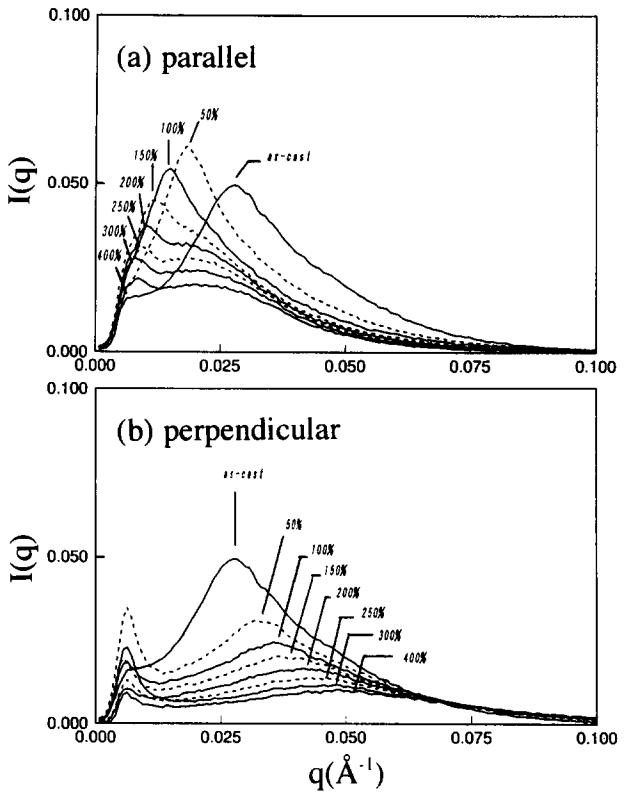

Figure 10 SAXS profiles of uniaxially stretched KP-13-3000 films at various strains. The scattering vector **q** is (a) parallel to the uniaxial strain (**q**∥ strain) and (b) perpendicular (**q**⊥ strain). Note that no correction for a change in thickness of the specimen was made in the scattered intensity

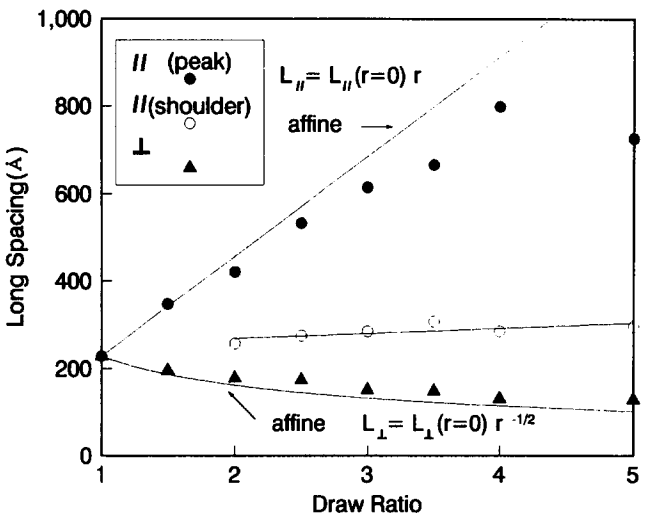

Figure 11 Plot of long spacing (L) against the draw ratio (r) for the uniaxially stretched KP-13-3000 films. The long spacing was calculated from the q value of the peak in the SAXS profile presented in *Figure 10* using Bragg's equation. The long spacing is calculated from the q values of the main peak for **q**∥ strain (●) and for **q** ⊥ strain (▲), and from the q value of the shoulder for **q**∥ strain (○). For the data represented by ● and ▲, the expected variations of $L(r)$ with respect to $L(r=0)$ are indicated by the solid curves by assuming the affine deformation

The change observed for the case of **q**⊥ strain is also presented in *Figure 10b*. Note that no correction for a change in thickness of the specimen was made in the scattered intensity. The peak shifts systematically towards the smaller angle region for the case of **q**∥ strain and towards the larger angle region for the case of **q**⊥ strain.

From 100% strain, a shoulder appeared at the larger angle beside the main peak for the case of **q**∥ strain, indicating that relaxation of the interdomain distance occurred partly in the specimen. This implies the dissociation of the hard-segment microdomains. In order to examine the relationship between the peak position and the strain, the long spacing is plotted against the draw ratio in *Figure 11*. The long spacing was calculated from the value of q at the peak using Bragg's equation. It is found that the affine deformation is more or less maintained below 100% strain. The long spacing calculated from the q value of the shoulder slightly increases with the draw ratio, indicating that the soft-segment chains which were relaxed by the dissociation of the hard-segment microdomains were restretched with the successive stretching. Thus, it is found for KP-13-3000 that the hard-segment microdomains were instantaneously dissociated by applying more than 100% of uniaxial static strain. Fakirov *et al.*[26] have reported a similar deformation behaviour with a uniaxial stretching observed for poly(ether ester) by SAXS.

Mechanism of changes in properties by fatigue

Since the SAXS experiments revealed that the dissociation of the hard-segment microdomains was induced by mechanical fatigue, the mechanism of changes in properties by the fatigue can be discussed in relation to the crystallization of the PTMG soft segments induced by the dissociation of the hard-segment microdomains. For KP-0-1000 and KP-13-1000, the mechanical properties hardly seemed to be affected by the fatigue. The soft segments could not crystallize, although the dissociation of the hard-segment microdomains was induced by the fatigue. This is due to the short block length of a soft segment ($M_{PTMG}=1000$) between hard segments which kinetically suppress the crystallization of the soft segments even in non-fatigued specimens[20]. As for KP-0-2000, the storage modulus in the region from -50 to 5°C increased, the peak height of $\tan\delta$ at $-40\sim-35$°C decreased and a distinct shoulder appeared at around -8°C. It was considered that the PTMG chains which were restrained from crystallizing by the hard-segment microdomains in the as-cast film became mobile enough to crystallize due to the dissociation of the hard-segment microdomains by the fatigue. On the other hand, no obvious change was observed in the mechanical properties of the fatigued KP-13-2000. This is explained by the effect of the PES components which lower the crystallizability of the soft segment even if the soft segments were released from constraint of the hard-segment microdomains[20]. Finally, for KP-0-3000 and KP-13-3000, the mechanical properties changed drastically due to fatigue, as a result of the crystallization of the soft segment triggered by the dissociation of the hard-segment microdomains. Although KP-13-3000 contains the PES component which has the ability to suppress the crystallization of the soft segments, the relatively long block length of the soft segment ($M_{PTMG}=3000$) may be advantageous for its crystallization.

CONCLUSION

As already reported[20], the non-fatigued KP-13-2000 has antithrombogenicity, due to the PES components, together with the elastomeric properties required for

biomedical materials. It was found in this study that KP-13-2000 has resistance against mechanical fatigue as well, which is one of the most important characteristics required for biomedical materials. Although the dissociation of the hard segment microdomain was induced by fatigue, the crystallization of the soft segments was prevented by the PES components and hence the mechanical properties of KP-13-2000 did not change owing to mechanical fatigue.

ACKNOWLEDGEMENTS

The authors are grateful to Professor Kanji Kajiwara and Dr Hiroshi Urakawa at the Department of Chemistry and Materials Technology, Kyoto Institute of Technology, Kyoto, and Professor Katsumi Kobayashi at the Photon Factory of the National Laboratory for High Energy Physics, Tsukuba, for their technical support on the SAXS measurements and the maintenance of the BL-10C beam line at the Photon Factory. This work has been performed with the approval of the Photon Factory Program Advisory Committee (Proposal no. 91-218). They are grateful to Dr Hiramatsu, Central Research, Kanegafuchi Chemical Industry Co. Ltd, Kobe, Japan, for supplying the samples. They acknowledge the financial support of the Resources and Environment Protection Research Laboratory, NEC Corporation, Kawasaki, Japan and are also indebted to Professor Tamotsu Hashimoto at the Department of Materials Science and Engineering, Fukui University for the g.p.c. measurements of the PTMG prepolymers.

REFERENCES

1 Planck, H., Egbers, G. and Syre, I. 'Polyurethanes in Biomedical Engineering', Elsevier, Amsterdam, The Netherlands, 1984
2 Lelah, M. D. and Cooper, S. L. 'Polyurethanes in Medicine', CRC Press, Boca Raton, FL, 1986
3 Clogh, S. B. and Schneider, N. S. *J. Macromol. Sci., Phys.* 1968, **B2**, 553
4 Huh, D. S. and Cooper, S. L. *Polym. Eng. Sci.* 1971, **11**, 36
5 Kimura, I., Ishihara, H., Ono, H., Yoshihara, N., Nomura, S. and Kawai, H. *Macromolecules* 1974, **7**, 355
6 Takahara, A., Tashita, J., Kajiyama, T. and Takayanagi, M. *Kobunshi Ronbunshu* 1982, **39**, 203
7 Hoffman, K. and Bonart, R. *Makromol. Chem.* 1983, **184**, 1529
8 Koberstein, J. T. and Stein, R. S. *J. Polym. Sci., Polym. Phys. Edn* 1983, **21**, 1439
9 Ishihara, H., Kimura, I. and Yoshihara, N. *J. Macromol. Sci., Phys.* 1983–1984, **B22**, 713
10 Miller, J. A., Lin, S. B., Hwang, K. K. S., Wu, K. S., Gibson, P. E. and Cooper, S. L. *Macromolecules* 1985, **18**, 32
11 Takahara, A., Tashita, J., Kajiyama, T., Takayanagi, M. and MacKnight, W. J. *Polymer* 1985, **26**, 978
12 Takahara, A., Tashita, J., Kajiyama, T., Takayanagi, M. and MacKnight, W. J. *Polymer* 1985, **26**, 987
13 Takahara, A. and Kajiyama, T. *Kobunshi Ronbunshu* 1985, **42**, 793
14 Shibayama, M., Kawauchi, T., Kotani, T., Nomura, S. and Matsuda, T. *Polym. J.* 1986, **18**, 719
15 Shibayama, M., Ohki, Y., Kotani, T. and Nomura, S. *Polym. J.* 1987, **19**, 1067
16 Yamamoto, T., Shibayama, M. and Nomura, S. *Polym. J.* 1989, **21**, 895
17 Kawano, S., Shibayama, M. and Nomura, S. *Rep. Prog. Polym. Phys. Jpn* 1990, **33**, 319
18 Li, C. and Cooper, S. L. *Polymer* 1990, **31**, 3
19 Shibayama, M., Inoue, M., Yamamoto, T. and Nomura, S. *Polymer* 1990, **31**, 749
20 Shibayama, M., Suetsugu, M., Sakurai, S., Yamamoto, T. and Nomura, S. *Macromolecules* 1991, **24**, 6254
21 Kira, K., Minokami, T., Yamamoto, N., Hayashi, K. and Yamashita, I. *Seitaizairyo* (*Biomaterials*) 1983, **1**, 29
22 Ueki, T., Hiragi, Y., Kataoka, M., Inoko, Y., Amemiya, Y., Izumi, Y. *et al. Biophys. Chem.* 1985, **23**, 115
23 Tran-Cong, Q., Kawakubo, R. and Sakurai, S. *Polymer* in press
24 McKenna, L. W., Kajiyama, T. and MacKnight, W. J. *Macromolecules* 1969, **2**, 58
25 Kajiyama, T. and MacKnight, W. J. *Macromolecules* 1969, **2**, 254
26 Fakirov, S., Fakirov, C., Fischer, E. W. and Stamm, M. *Polymer* 1991, **32**, 1173